HHS Public Access

Author manuscript

Anesthesiology. Author manuscript; available in PMC 2017 November 01.

Published in final edited form as:

Anesthesiology. 2016 November ; 125(5): 929–942. doi:10.1097/ALN.0000000000001342.

Neural Correlates of Wakefulness, Sleep, and General Anesthesia: An Experimental Study in Rat

Dinesh Pal, Ph.D.[1,2], **Brian H. Silverstein, B.A.**[2,3], **Heonsoo Lee, Ph.D.**[1], and **George A. Mashour, M.D., Ph.D.**[1,2,4,*]

[1]Department of Anesthesiology, University of Michigan, 7433 Medical Science Building I, 1150 West Medical Center Drive, Ann Arbor, MI 48109-5615

[2]Center for Consciousness Science, University of Michigan, Ann Arbor, MI 48109

[3]Translational Neuroscience Program, Wayne State University School of Medicine, Tolan Park Medical Building Suite 5-B, 3901 Chrysler Service Drive, Detroit, MI 48201

[4]Neuroscience Graduate Program, University of Michigan, Ann Arbor, MI 48109

Abstract

Background—Significant advances have been made in our understanding of subcortical processes related to anesthetic- and sleep-induced unconsciousness, but the associated changes in cortical connectivity and cortical neurochemistry have yet to be fully clarified.

Methods—Male Sprague-Dawley rats were instrumented for simultaneous measurement of cortical acetylcholine and electroencephalographic indices of corticocortical connectivity - coherence and symbolic transfer entropy - before, during, and after general anesthesia (propofol, n=11; sevoflurane, n=13). In another group of rats (n=7), these electroencephalographic indices were analyzed during wakefulness, slow wave sleep (SWS), and rapid eye movement (REM) sleep.

Results—Compared to wakefulness, anesthetic-induced unconsciousness was characterized by a significant decrease in cortical acetylcholine that recovered to pre-anesthesia levels during recovery wakefulness. Corticocortical coherence and frontal-parietal symbolic transfer entropy in high gamma band (85-155 Hz) were decreased during anesthetic-induced unconsciousness, and returned to pre-anesthesia levels during recovery wakefulness. Sleep-wake states showed a state-dependent change in coherence and transfer entropy in high gamma bandwidth, which correlated with behavioral arousal: high during wakefulness, low during SWS, and lowest during REM sleep. By contrast, frontal-parietal theta connectivity during sleep-wake states was not correlated with behavioral arousal but showed association with well-established changes in cortical acetylcholine: high during wakefulness and REM sleep, and low during SWS.

*To whom correspondence should be addressed: gmashour@med.umich.edu, Department of Anesthesiology, University of Michigan Medical School, 1H247 University Hospital, SPC-5048, 1500 E. Medical Center Drive, Ann Arbor, MI 48109-5048, Phone: 1-734-936-4280, Fax: 1-734-936-9091 .

Conflict of interest: The authors declare no competing financial interests.

Conclusion—Corticocortical coherence and frontal-parietal connectivity in the high gamma bandwidth correlates with behavioral arousal and is not modulated by cholinergic mechanisms, while theta connectivity correlates with cortical acetylcholine levels.

Introduction

The neural correlates of anesthetic- and sleep-induced unconsciousness have yet to be fully clarified, but growing evidence suggests that fragmentation of cortical networks consistently occurs during pharmacological, physiological, and pathological states of unconsciousness. Anesthetics with diverse molecular profiles and neurophysiological effects have been shown to fragment functional networks in the cortex,[1-5] and both sleep and anesthesia reduce surrogates of cortical information transfer.[4-12] Several recent studies encourage further investigation of the role of cortex in anesthetic-induced unconsciousness. First, in rats, cross-modal cortical interactions are more sensitive to anesthetic effects than first-order thalamocortical circuits.[13] Second, in humans, disrupted corticocortical connectivity has been reported to better distinguish propofol-induced unconsciousness from wakefulness and sedation compared with changes in thalamocortical connectivity.[14,15] Although correlative, these findings are mechanistically relevant given the apparent requirement for integration of cortical networks during normal conscious experience.[16,17] Furthermore, the relationship of anesthetic- and sleep-induced unconsciousness is a subject of active exploration,[18-25] but systematic comparisons of brain connectivity changes during anesthetic- (intravenous as well as inhaled) and sleep-induced unconsciousness have been lacking. Finally, despite the focus on functional, directed, and effective connectivity changes during general anesthesia,[26] there is little understanding of the underlying neurochemical control of connectivity patterns, which might provide an explanatory link to the molecular actions of general anesthetics.

In this study, we investigated the relationship of cortical acetylcholine and measures of brain connectivity - coherence and symbolic transfer entropy - derived from the electroencephalogram under multiple conditions: 1) before, during, and after unconsciousness induced by propofol or sevoflurane, 2) during spontaneous wakefulness, 3) during slow wave sleep (SWS), and 4) during rapid eye movement (REM) sleep. We report that electroencephalographic coherence and frontal-parietal directed connectivity in the high gamma (85-155 Hz) bandwidth is present during wakefulness and disrupted during physiological (SWS and REM sleep) and pharmacological (propofol and sevoflurane) states of unconsciousness. By contrast, coherence and bidirectional frontal-parietal connectivity in the theta bandwidth are present during states of cortical activation (low amplitude- fast wave electroencephalogram) with (wakefulness) or without (REM sleep) behavioral arousal, and correlate with cortical acetylcholine levels. We conclude that coherence and frontal-parietal directed connectivity in high gamma band are neural correlates of wakefulness that are not mediated by cholinergic mechanisms.

Materials and Methods

All experiments were conducted on adult male Sprague-Dawley rats (n=31, 300-350 g, Charles River Laboratories Inc., MA). The rats were housed in a temperature-controlled facility with 12 h light: 12 h dark cycle (lights on at 6:00 am) and *ad libitum* access to food

and water. The experimental procedures were approved by the Institutional Animal Care and Use Committee at the University of Michigan (Ann Arbor, Michigan, USA), and were in compliance with the Guide for the Care and Use of Laboratory Animals (8th Edition, The National Academies Press, Washington D.C.) as well as ARRIVE guidelines.

Surgical procedures

Rats were anesthetized with 3-4% isoflurane in 100% oxygen and positioned in a stereotaxic frame (Model 963, David Kopf Instruments, Tujunga, CA) using blunt ear bars. Isoflurane (1-2%) was delivered through a rat anesthesia mask (Kopf Model 906) and was titrated to effect during surgery. General anesthesia was assessed by the absence of pedal and palpebral reflex. An anesthetic agent analyzer (Datex Medical Instrumentation, Inc., Tewksbury, MA) was used for continuous monitoring of delivered isoflurane concentration. Core body temperature was monitored using a rectal probe (Model 7001H, Physitemp Instruments, Inc., Clifton, New Jersey). A small animal far-infrared heating pad (Kent Scientific Co., Torrington, Connecticut) was used for the maintenance of body temperature at 37.0 ± 1 °C. All rats (n=31) were implanted with stainless steel screw electrodes to record electroencephalogram from 1) frontal cortex: anterior-posterior = + 3.0 mm, medial-lateral = 2.5 mm, 2) parietal cortex: anterior-posterior = −4.0 mm, medial-lateral = ± 2.5 mm, and 3) occipital cortex: anterior-posterior = − 8.0 mm, medial-lateral = ± 2.5 mm, and a screw electrode over the nasal sinus to serve as the reference electrode; all coordinates were with respect to Bregma. In a sub-group of these rats (n=7), multi-stranded insulated (except at the tips) wires (AS636, Cooner Wires, Inc., Chatsworth, CA) were implanted in the dorsal neck muscles for recording electromyogram. These rats were used for recording sleep-wake states. All other rats (n=24) were implanted with a CMA/11 microdialysis guide cannula (CMA Microdialysis, Harvard Apparatus, Holliston, MA) aimed at 1.0 mm above prefrontal cortex (PFC) (anterior-posterior = + 3.0 mm, medial-lateral = 0.5 mm, ventral = 4.0 mm)[27] for microdialysis measurement of acetylcholine levels. The electrodes were interfaced with six-pin pedestal(s) (MS363, Plastics One, Roanoke, VA) and the entire assembly along with microdialysis guide cannula was secured with dental cement (Cat No. 51459, Stoelting Co, Woodlake, IL). A sub-group of rats (n=11) with the electrodes for electroencephalographic recording and microdialysis guide tube was implanted with an indwelling catheter (Micro-Renathane tubing, MRE-040, Braintree Scientific, MA) in the internal jugular vein to provide access for propofol infusion. The catheter was tunneled under the skin and mated with a port (313-000BM-10, Plastics One, Roanoke, VA) sutured on the back muscles between the scapulae. The remaining rats (n=13) with the electrodes for electroencephalographic recording and microdialysis guide tube but without intravenous catheter were used for sevoflurane experiments. Buprenorphine hydrochloride (Buprenex ®, Reckitt Benckiser Pharmaceuticals Inc., Richmond, VA) was used for pre-surgical (0.01 mg kg^{-1}, s.c.) and post-surgical (0.03 mg kg^{-1}, s.c., every 8-12 hours for 24 hours) analgesia and all rats received a single pre-surgical dose (20 mg kg^{-1}, s.c.) of antibiotic cefazolin (West-Ward-Pharmaceutical Corp., Eatontown, NJ). The rats implanted with catheters received an additional dose of antibiotic gentamicin (5.0 mg kg^{-1} body wt, i.v.) during the surgery. Animals were kept under observation until ambulatory and then returned to their home cage for post-surgical recovery. All rats were provided at least 7-10 days of post-surgical recovery during which they were conditioned to the recording chamber and cables.

The jugular venous catheter was flushed with 0.3 mL of heparinized saline (1 unit mL^{-1}, Sagent Pharmaceuticals, Schaumburg, IL) every other day.

Microdialysis quantification of acetylcholine using high performance liquid chromatography (HPLC) coupled with electrochemical detection

Microdialysis samples were collected every 12.5 min (25 μL) with CMA/11 microdialysis probes (1 mm cuprophane membrane, 0.24 mm diameter, 6 kD), which were perfused continuously with Ringer's solution (147 mM NaCl, 2.4 mM $CaCl_2$, 4.0 mM KCl, 10 μM neostigmine; pH 6.0 ± 0.2) at 2.0 μL min^{-1} using a CMA/400 syringe pump (CMA Microdialysis, Harvard Apparatus, Holliston, MA). From each microdialysis sample, 22 μL was injected into a HPLC paired with an electrochemical detector (Bioanalytical Systems, West Lafayette, IN) for acetylcholine quantification. An ion-exchange (mobile phase: 50 mM Na_2HPO_4, pH 8.5) analytical column (MF-6150, Bioanalytical Systems, West Lafayette, IN) separated acetylcholine and choline in the dialysis samples, which were proportionately catalyzed into hydrogen peroxide by an immobilized enzyme reactor column (MF-6151, Bioanalytical Systems, West Lafayette, IN). Hydrogen peroxide was detected by oxidation (applied potential at 500 mV, Ag^+/AgCl reference electrode) at a platinum working electrode. The chromatograms were digitized to quantify acetylcholine level using ChromGraph software (Bioanalytical Systems, West Lafayette, IN) and a 7-point standard curve (0.05-1.0 pmol).

Electrophysiological data acquisition

The electrophysiological signals were amplified with a Grass Model 15 LT bipolar portable physiodata amplifier system (15A54 Quad Amplifier, Natus Neurology Inc., Warwick, RI). A MP150 data acquisition unit along with Acq*knowledge* software (version 4.1.1, Biopac Systems, Inc, Goleta, CA) was used for digitizing and storing the data. The electrode implanted over nasal sinus served as the reference for recording monopolar electroencephalogram (0.1-300 Hz, 1 kHz sampling rate) from frontal, parietal, and occipital cortices, which were used for connectivity analyses. Bipolar electroencephalogram (frontal-parietal and parietal-parietal, 0.1-100 Hz, 250 Hz sampling rate) and electromyogram (1-100 Hz, 250 Hz sampling rate) were recorded for quantification of sleep-wake states. Electroencephalogram signals were amplified 5000 times while electromyogram signals were amplified 10,000 times.

Corticocortical coherence and directed connectivity analysis

The data were first down-sampled to 500 Hz to reduce computation time and an IIR notch filter was applied to remove 60 Hz line noise. Magnitude squared coherence was calculated at individual frequencies in 0.5 Hz intervals from 0.5 to 155 Hz between all electrode pairs in 2 s moving windows using the 'mscohere.m' function in the MATLAB Signal Processing Toolbox (MathWorks Inc., Natick, MA, USA). Using the approach demonstrated in previous publications from our[28,29] and other laboratories,[30,31] the coherence values were averaged over the following frequency bands: delta (δ: 0.5-4 Hz), theta (θ: 4-10 Hz), alpha (α: 10-15 Hz), beta (β: 15-25 Hz), low gamma (γ1: 25-55 Hz), medium gamma (γ2: 85-125 Hz), and high gamma (γ3: 125-155 Hz). The mean global coherence was obtained by averaging the coherence for individual channel pairs for each animal. To control for the possibility of

spurious coherence affecting the analysis, the empirical data were statistically compared with a surrogate data set in which the phase relationships between the electroencephalogram signals were disrupted without altering the spectral content of each signal.[32] Paired t test showed a significant difference ($p < 0.000001$) in the coherence between the empirical and surrogate data sets, confirming that the measured coherence was not accounted for merely by spectral shifts of the signal across states.

We used normalized symbolic transfer entropy (NSTE) to assess directional connectivity. NSTE is an information theoretic measure and serves as a surrogate for directed cortical communication. Our previous studies have validated the use of NSTE to measure connectivity changes in humans[7,8,11] and rats,[28] and other laboratories have supported our findings with NSTE using different approaches - functional connectivity and dynamic causal modeling.[9,14] Transfer entropy, the basis of NSTE, was also used in a previous study of evoked potentials in low gamma range (≤50 Hz) in rats[33] and head-restrained ferrets.[34] We selected theta and gamma band for NSTE analysis because these have been linked to electroencephalographic activation, changes in cortical acetylcholine, and changes in states of behavioral arousal and consciousness.[29,35] NSTE was analyzed between frontal-parietal areas because studies from human volunteers, patients, and animals suggest the importance of frontal-parietal networks in consciousness of the environment.[7,8,9,11,14,26,33,36] NSTE was calculated between left frontal and left parietal areas in theta (θ: 4-10 Hz), low gamma (γ1: 25-55 Hz), medium gamma (γ2: 85-125 Hz), and high gamma (γ3: 125-155 Hz) bands as has been described previously.[11,28] In brief, sampling rate was kept at 1 kHz to improve the stability of the analysis. The continuous raw electroencephalographic data were first filtered for the frequency band of interest (theta, low gamma, medium gamma, and high gamma) with a zero phase FIR filter of order 400 designed using firls2.m (MATLAB Signal Processing Toolbox) and implemented using filtfilt.m (MATLAB Signal Processing Toolbox). Data were then extracted from time periods of interest and analyzed in 10 s bins. Note that all electroencephalographic analyses were performed on the same data epochs. NSTE requires three parameters: embedding dimension (d_E), time delay (τ), and prediction time (δ). These parameters were selected such that the transfer entropy from the source signal to the target signal was maximized for a given data window, as described previously.[11,28] In brief, d_E was kept fixed at 3, δ was set by selecting the lag that maximized the cross-correlation between the two signals, and τ was varied from 1 to 30. The potential bias of STE was removed using a shuffled data set, after which the unbiased data set was normalized.[11,28]

Simultaneous electroencephalographic recordings and microdialysis measurement of changes in acetylcholine levels before, during, and after propofol- and sevoflurane-induced unconsciousness

The rats were connected to the electroencephalogram recording system at least 30 min prior to the start of experimental session (9:30 am-10:00 am) and a microdialysis probe being infused with Ringer's solution at 2.0 μL min^{-1} was lowered into the PFC. Electroencephalogram was recorded continuously while the microdialysis samples were collected every 12.5 min throughout the experiment. Previous reports from our[29] and other[37] laboratories have shown that it takes up to 37.5 min for the *in vivo* baseline acetylcholine

levels to stabilize after the probe insertion. Therefore, the first three microdialysis samples were excluded and six pre-anesthesia baseline microdialysis samples were collected. In order to hold the behavioral state constant during the baseline condition, the rats were kept awake using gentle tapping on the recording chamber. At the completion of six wake microdialysis samples, the rats were either connected to a micro-syringe pump (SP 101I, WPI Inc., Sarasota, FL) through the venous catheter for continuous intravenous propofol infusion (800 μg $kg^{-1}min^{-1}$) or were exposed to sevoflurane anesthesia (2.0-2.2 %), and six microdialysis samples were collected during administration of the anesthetic. Sevoflurane experiments were conducted in a custom-made clear round recording chamber, which could be rotated in a direction opposite to that of the rat's movement. This apparatus allows the rat to stay in the center of the chamber, thereby preventing any kinks in the microdialysis tubing. The recording chamber can be sealed during anesthesia and was fitted with a door to allow access to the animal during anesthetic exposure. The chamber also had ports for inlet and outlet of anesthetic vapors, which were monitored using two anesthetic agent analyzers (Datex Medical Instrumentation, Inc., Tewksbury, MA). The anesthetic concentration was based on preliminary experiments conducted in our laboratory and was titrated to produce loss of righting reflex (LORR) along with slow wave (high-amplitude delta waves) electroencephalogram, both of which are used as a surrogate for loss of consciousness.[38,39] Propofol and sevoflurane produced LORR within about 20 min, after which the rats were maintained in a recumbent position for the rest of the anesthetic administration. The core body temperature was monitored and maintained at 37.0 ± 1 °C using a far-infrared heating pad. At the completion of six microdialysis samples during administration of the anesthetic, the propofol infusion/sevoflurane exposure was stopped. Thereafter, six microdialysis samples were collected in the post-sevoflurane recovery period. Initial experiments with propofol (n=3) showed that the acetylcholine levels during post-propofol recovery period (6 microdialysis samples) remained below baseline wake levels. The data from these initial propofol experiments, which only had six post-propofol recovery samples, were excluded from the analysis. In addition, it took much longer for the rats to recover righting reflex after propofol anesthesia (~29 min) as compared to sevoflurane (<10 min), which likely reflects pharmacokinetics. Therefore, in order to ensure a complete recovery from the effects of propofol anesthesia, microdialysis samples were collected for an extended recovery period (12 microdialysis samples) in the remaining eight rats. In the propofol group, we could not collect microdialysis samples in one out of the eight rats with extended recovery period because of microdialysis probe malfunction. In the sevoflurane group, two rats did not have good electroencephalogram signals and the microdialysis probe failed in one of the rats. The last epoch during wake, anesthetic-induced unconsciousness, and post-anesthetic recovery period was taken as the most stable and representative of the corresponding states, and therefore the electroencephalogram and acetylcholine analysis was restricted to these 12.5 min epochs.

Polysomnographic recordings and quantification of sleep-wake states

Monopolar (frontal, parietal, and occipital cortices) and bipolar electroencephalogram (frontal-parietal and parietal-parietal) along with electromyogram were recorded for 12 h between 6:00 am and 6:00 pm during the light phase. Bipolar electroencephalogram and electromyogram in 10 s bins were used for the characterization and quantification of wake

(low amplitude-fast wave electroencephalogram with high muscle tone), slow wave sleep (SWS) (high amplitude-slow wave electroencephalogram with low muscle tone), and rapid eye movement (REM) sleep (low amplitude-fast wave electroencephalogram along with muscle atonia). Only pure sleep or wake epochs were selected for the analysis i.e., wakefulness epoch was characterized by the presence of low amplitude-fast wave electroencephalogram and high muscle tone for 100% of the time in the 10 s epoch. Similarly, for REM sleep, the selected epochs were characterized by low amplitude-fast wave electroencephalogram and muscle atonia for 100% of the time in 10 s epoch. Selection of these pure epochs ensured that there was no potential confound in the connectivity analysis arising from mixed states within a single epoch. Out of a total of 4320 ten second epochs, we selected a subset of 99 pure epochs for connectivity analysis. Note that the state of wakefulness in these experiments was spontaneous, while the state of baseline wakefulness in the study of propofol- and sevoflurane-induced unconsciousness was maintained by the experimenters.

Histological confirmation of the microdialysis sites

After 3-7 days of microdialysis and electroencephalogram data collection, rats were deeply anesthetized (ketamine - xylazine: 80 mg kg^{-1} - 10 mg kg^{-1} body wt, i.p.) and transcardially perfused with 100 mL of phosphate buffered saline (0.1 M, pH 7.2; 1219SK, EM Sciences, Hatfield, PA) followed by 250 mL of fixative (4% paraformaldehyde, 4% sucrose, 0.1 M phosphate buffer, pH 7.2; 1224SK, EM Sciences, Hatfield, PA) solution. The brains were extracted and stored in a fixative solution for at least 24 h and then allowed to equilibrate in 30% sucrose in phosphate buffer. Forty micron coronal sections were cut through the PFC on a cryostat (Leica Microsystems Nussloch GmbH, Nussloch, Germany). The sections were mounted on slides and stained with cresyl violet to confirm the site of microdialysis.

Statistical analyses

Statistical analyses were conducted in consultation with the Center for Statistical Consultation and Research at the University of Michigan. *A Priori* power analysis (nQuery Advisor + nTerim, Statistical Solutions Ltd, MA) using the acetylcholine pilot data indicated that a minimum sample size of 3 would have 80% power (effect size = 4.0) to detect a difference in means of 0.8 pmole (standard deviation of difference = 0.2); paired t test with one-sided alpha = 0.05/3 (Bonferroni correction for 3 pairwise tests). All statistical comparisons were conducted in a within-group design and a p value of <0.05 was considered statistically significant. Each group of rats in this study had different surgical implants - jugular venous catheter and microdialysis probe in propofol group, microdialysis probe without jugular venous catheter in sevoflurane group, and neither catheter nor microdialysis probe in sleep-wake group. Therefore, random allocation of rats to different experimental conditions was not possible. Additionally, the experimenters could not be blinded to the experiments because the experimental interventions (propofol infusion, sevoflurane exposure, and sleep-wake recordings) were clearly different and could not be masked. Repeated measures analysis of variance (RMANOVA) with Tukey's multiple comparisons test was used for the comparison of acetylcholine levels as well as the electroencephalographic coherence in each frequency band between the last epochs from the periods of 1) wakefulness, 2) anesthetic-induced unconsciousness (propofol and

sevoflurane), and 3) post-anesthetic recovery wakefulness. These epochs were also used for the comparison of directed connectivity between frontal and parietal areas for theta and gamma (low, medium, and high) bands. Similarly, RMANOVA with Tukey's post-hoc test was used for the comparison of coherence and directed connectivity during sleep-wake states. The data are reported as mean ± standard error of the mean (s.e.m.) along with 95% confidence interval (CI). To enhance readability, only p values are provided in the results section while mean ± s.e.m., 95% confidence interval and F statistic are provided in a tabular format **(see** tables 1-5 for descriptive and inferential statistics, Supplemental Digital Content 1**)**. Statistical comparisons were performed with Graph Pad Prism 6.05 (Graph Pad Software, Inc., La Jolla, CA).

Results

Cortical acetylcholine across multiple states of arousal

The temporal course of the changes in PFC acetylcholine levels before, during, and after anesthetic-induced unconsciousness is illustrated in figure 1A. Histological analysis confirmed the probe placement in the PFC for all the rats in propofol and sevoflurane groups **(**fig. 1B and 1C**)**. The effect of propofol and sevoflurane on cortical acetylcholine is shown in figure 2 and 3, respectively. There was a statistically significant decrease in acetylcholine levels during propofol- (p=0.005) and sevoflurane- (p=0.0006) induced unconsciousness as compared to the waking state **(**fig. 2A **and** 3A, **See** table 1 for descriptive and inferential statistics, Supplemental Digital Content 1**)**. The decrease in acetylcholine was comparable between propofol (~90%) and sevoflurane (~85%) groups. Compared to anesthetic-induced unconsciousness, the recovery wake epoch for both propofol (p=0.004) and sevoflurane (p=0.002) groups was characterized by a significant increase in acetylcholine levels that was not statistically different from pre-anesthesia wake acetylcholine levels **(**fig. 2A **and** 3A**, See** table 1 for descriptive and inferential statistics, Supplemental Digital Content 1**)**. Previous reports have demonstrated that cortical acetylcholine levels are high during wakefulness, low during SWS, and high again during REM sleep, approximating the levels observed during wake state.[35,40] These changes in cortical acetylcholine across sleep-wake states have been well described and accepted. Therefore, we did not measure changes in cortical acetylcholine during sleep-wake states in the current study.

Electroencephalographic coherence and directed connectivity before, during, and after anesthetic-induced unconsciousness

The decrease in acetylcholine levels in PFC during anesthetic-induced unconsciousness was associated with a reduction in long-range corticocortical coherence **(**fig. 2B **and** 3B**, See** table 2 for descriptive and inferential statistics, Supplemental Digital Content 1**)**. As compared to wakefulness, anesthetic-induced unconsciousness produced a significant decrease in electroencephalographic coherence in delta (propofol: p=0.001, sevoflurane: p=0.004), theta (propofol: p=0.0004, sevoflurane: p=0.003), alpha (propofol: p=0.0004, sevoflurane: p=0.006), beta (propofol: p=0.0003, sevoflurane: p=0.0006), low gamma (propofol: p<0.0001, sevoflurane: p<0.0001), medium gamma (propofol: p<0.0001, sevoflurane: p<0.0001), and high gamma (propofol: p=0.0002, sevoflurane: p<0.0001) bands **(**fig. 2B **and** 3B**, See** table 2 for descriptive and inferential statistics, Supplemental

Digital Content 1**)**. Compared to anesthetic-induced unconsciousness, coherence during the recovery wake epoch showed a significant increase and returned to wake levels in all bands except delta band in the propofol and sevoflurane groups: delta (propofol: p=0.08, sevoflurane: p=0.05), theta (propofol: p=0.001, sevoflurane: p=0.03), alpha (propofol: p=0.0002, sevoflurane: p=0.02), beta (propofol: p=0.0007, sevoflurane: p=0.004), low gamma (propofol: p<0.0001, sevoflurane: p<0.0001), medium gamma (propofol: p=0.0004, sevoflurane: p=0.0006), and high gamma (propofol: p=0.003, sevoflurane: p=0.0002); delta coherence during recovery from sevoflurane-induced unconsciousness remained significantly lower as compared to that observed during the wake state (p=0.01) **(**fig. 2B **and** 3B**, See** table 2 for descriptive and inferential statistics, Supplemental Digital Content 1**)**. The effect of general anesthetics on cortical coherence was driven by similar changes in the coherence in individual channel pairs across the cortex **(See** fig. 1 and 2, Supplemental Digital Content 2**)**.

Next, we analyzed NSTE between left frontal and left parietal cortices in theta and gamma bands before, during, and after anesthetic-induced unconsciousness. As compared to wakefulness, propofol-induced unconsciousness was marked by a significant decrease in frontal-to-parietal connectivity in theta (p=0.02) and gamma (low: p=0.003, medium: p<0.0001, high gamma: p=0.0001) bands (fig. 2C**, See** table 3 for descriptive and inferential statistics, Supplemental Digital Content 1**)**. The parietal-to-frontal connectivity also decreased in theta (p=0.02), medium gamma (p=0.0004), and high gamma (p=0.0002) bands while there was no statistically significant change in low gamma band (p=0.1) **(**fig. 2D**, See** table 3 for descriptive and inferential statistics, Supplemental Digital Content 1**)**. As compared to propofol-induced unconsciousness, the connectivity during post-propofol recovery epoch in both directions in theta (frontal-to-parietal: p=0.0004, parietal-to-frontal: p=0.01), medium gamma (frontal-to-parietal: p=0.003, parietal-to-frontal: p=0.01), and high gamma (frontal-to-parietal: p=0.004, parietal-to-frontal: p=0.004) bands showed a significant increase and returned to the pre-anesthesia wake levels. The group-level statistical changes in medium and high gamma frontal-parietal connectivity were supported by changes in connectivity in each individual rat; all rats showed a decrease in frontal-parietal connectivity in medium and high gamma bands. The response was more variable in the low gamma band. Sevoflurane-induced unconsciousness was also marked by a decrease in frontal-to-parietal connectivity in gamma bands (low: p=0.01, medium: p=0.0009, high: p<0.0001) **(**fig. 3C**, See** table 3 for descriptive and inferential statistics, Supplemental Digital Content 1**)**. There was no significant change in frontal-to-parietal theta connectivity (p=1.0) during sevoflurane-induced unconsciousness as compared to wakefulness. The parietal-to-frontal connectivity decreased in theta (p=0.003) and higher gamma bands (medium: p=0.0004, high: p<0.0001) while there was no statistically significant change in low gamma band (p=0.4) **(**fig. 3D**, See** table 3 for descriptive and inferential statistics, Supplemental Digital Content 1**)**. Compared to sevoflurane-induced unconsciousness, bidirectional connectivity increased in medium (frontal-to-parietal: p=0.01, parietal-to-frontal: p=0.01) and high (frontal-to-parietal: p=0.0003, parietal-to-frontal: p=0.0005) gamma bands during the post-sevoflurane recovery wake epoch and returned to the pre-sevoflurane wake levels. Frontal-to-parietal theta connectivity was significantly higher during post-sevoflurane recovery wake epoch as compared to pre-sevoflurane wake (p=0.04) as well as the

unconscious state (p=0.02) while parietal-to-frontal theta connectivity showed an increase (p<0.0001) during post-sevoflurane recovery wake epoch and returned to the pre-sevoflurane wake levels.

Electroencephalographic coherence and directed connectivity during sleep-wake states

As compared to wakefulness, SWS was characterized by a significant decrease in corticocortical coherence in delta (p<0.0001), theta (p=0.0001), alpha (p=0.007), medium gamma (p=0.0002), and high gamma (p=0.0001) bands; there was no statistical difference in coherence in beta (p=0.07) and low gamma (p=0.2) bands **(**fig. 4A**, See** table 4 for descriptive and inferential statistics, Supplemental Digital Content 1**)**. Compared to SWS, corticocortical coherence decreased during REM sleep in beta (p=0.0004) and gamma range (low: p=0.001, medium: p=0.0004, high: p=0.008) while it increased in theta (p<0.0001) and alpha (p=0.0001) bands **(**fig. 4A**, See** table 4 for descriptive and inferential statistics, Supplemental Digital Content 1**)**. There was no significant difference (p=0.2) in delta coherence between SWS and REM sleep. Compared to wakefulness, REM sleep was characterized by reduced coherence in delta (p<0.0001), beta (p=0.004), and the entire gamma range (low: p=0.0001, medium: p<0.0001, high: p<0.0001); there was no significant difference in theta (p=0.2) and alpha (p=0.6) bands between wakefulness and REM sleep **(**fig. 4A**, See** table 4 for descriptive and inferential statistics, Supplemental Digital Content 1**)**. Global changes in cortical coherence during sleep-wake states were also evident in the changes in coherence observed in individual channel pairs across the cortical areas **(See** fig. 3, Supplemental Digital Content 2**)**.

Bidirectional frontal-parietal connectivity in theta band **(**fig. 4B and 4C**)** followed a pattern that closely mirrored the cortical acetylcholine levels reported across sleep-wake states.[35,40] Compared to the wake state, frontal-parietal theta connectivity decreased during SWS (frontal-to-parietal: p=0.0006, parietal-to-frontal: p<0.0001) and increased during REM sleep (frontal-to-parietal: p=0.003, parietal-to-frontal: p=0.007) **(**fig. 4B and 4C**, See** table 5 for descriptive and inferential statistics, Supplemental Digital Content 1**)**. As opposed to frontal-parietal theta connectivity, the frontal-parietal connectivity in gamma range showed a progressive reduction from wake to REM sleep and did not mirror the known changes in cortical cholinergic tone **(**fig. 4B and 4C**)**. The frontal-to-parietal connectivity in medium (p=0.006) and high gamma (p=0.002) showed a significant decrease from wake to SWS, and all three gamma bands were significantly reduced during REM sleep as compared to both wake (low: p=0.009, medium: p=0.0007, high: p=0.0002) and SWS (low: p=0.01, medium: p=0.003, high: p=0.04). Frontal-to-parietal connectivity in low gamma band was not significantly different between wake and SWS (p=0.12) **(**fig. 4B**, See** table 5 for descriptive and inferential statistics, Supplemental Digital Content 1**)**. Similarly, as compared to wakefulness, the parietal-to-frontal connectivity in gamma bands decreased during SWS (low gamma: p=0.04, medium gamma: p=0.003, high gamma: p=0.0005) and during REM sleep (low gamma: p=0.009, medium gamma: p=0.0004, high gamma: p=0.0001). As compared to SWS, the parietal-to-frontal connectivity in medium gamma (p=0.002) and high gamma (p=0.009) decreased further during REM sleep; there was no statistical difference in low gamma between SWS and REM sleep (p=0.05) **(**fig. 4C**, See** table 5 for descriptive and inferential statistics, Supplemental Digital Content 1**)**. The group-level

statistical changes in medium and high gamma frontal-parietal connectivity were supported by changes in connectivity in each individual rat; all rats showed a decrease in frontal-parietal connectivity in medium and high gamma bands. The response was more variable in the low gamma band.

Discussion

In this study of multiple states of arousal, we demonstrate that corticocortical coherence and frontal-parietal directed connectivity in high gamma (85-155 Hz) range is a consistent neural correlate of wakefulness. Reduction of high gamma frontal-parietal directed connectivity was not simply found at a group level but in each animal under the state of anesthetic- or sleep-induced unconsciousness. Frontal-parietal connectivity in the low gamma (25-55 Hz) range showed similar patterns, but the response was not consistent across all animals studied. In contrast to frontal-parietal high gamma connectivity, frontal-parietal connectivity in the theta bandwidth was correlated with cholinergic tone in the presence (wakefulness) or absence (REM sleep) of behavioral arousal. The relationship between different electroencephalographic indices, cortical acetylcholine, and the behavioral states is summarized in Table 1.

Breakdown of high gamma corticocortical coherence during anesthesia and sleep

The emergence of cortical gamma oscillations has been posited to be a result of local interactions between inhibitory and excitatory processes – a reciprocal interaction between inhibitory fast spiking parvalbumin positive GABAergic neurons (interneuron-interneuron gamma or ING model) or the interaction of excitatory pyramidal neurons with these inhibitory neurons (pyramidal-interneuron gamma or PING model).[41-43] Human and animal studies have demonstrated both local and long range gamma synchronization across neuronal networks.[44-47] Earlier studies of low gamma oscillations (≤50 Hz) showed that anterior-posterior corticocortical phase synchronization in rats,[48] and coherence in surgical patients,[49] decreased under anesthetic-induced unconsciousness. In a recent study conducted in surgical patients, Nicolaou and Georgiou reported[30] that global field synchrony in gamma band was significantly reduced during surgical anesthesia with propofol, sevoflurane, and desflurane. Gamma coherence was also found to be disrupted during REM sleep in animals.[50-52] In this study, we confirmed these earlier findings and in addition demonstrated a decrease in high gamma (125-155 Hz) coherence during propofol- and sevoflurane-induced anesthesia as well as during SWS and REM sleep.

Disruption of high gamma frontal-parietal directed connectivity during anesthesia and sleep

The changes in coherence and similar phase-based measures of functional connectivity are indicative of statistical covariation in neural oscillations across the brain but do not provide any information on the influence of one brain region over another. Therefore, in order to gain insights into the information exchange between different cortical areas, we studied the effect of anesthetic- and sleep-induced unconsciousness on corticocortical directed connectivity. Past work in humans and animals supports a role for directed connectivity from frontal cortex to more posterior cortical areas in consciousness. In human volunteers and

surgical patients, we have demonstrated that three distinct general anesthetics selectively suppress anterior-to-posterior directed connectivity,[7,8,11] and related studies in human volunteers show that diverse anesthetics reduce the complexity of cortical response to perturbation with transcranial magnetic stimulation.[2,4] However, these studies were either restricted to a lower gamma range (because of the use of scalp electroencephalogram) or utilized a perturbational approach involving transcranial magnetic stimulation of cortex and measuring the spread of response as an index of brain connectivity. The current study in rats is the first study on spontaneous frontal-parietal connectivity across multiple states of arousal with an emphasis on the high gamma bandwidth. Our data confirm earlier reports from human and animal studies[7,8,11,14,33,34] that show a preferential inhibition of frontal-to-parietal connectivity during anesthesia in low gamma range, but in addition demonstrate for the first time that high gamma (85-155 Hz) frontal-parietal directed connectivity appears to be most consistently affected and closely correlated to loss of wakefulness during general anesthesia, SWS, and REM sleep. There are two major possibilities that account for this finding. The first is that there is a fragmentation of cortical networks, which confines information processing in the high gamma bandwidth to a modular network that cannot effectively communicate. The second possibility - not mutually exclusive - is that information processing itself is diminished even within the local modules. Discriminating among these possibilities depends, in part, on the direction of the connectivity and the oscillation bandwidths. For example, parietal-to-frontal connectivity is preserved in the low gamma bandwidth during anesthetic-induced unconsciousness and correlates with visual sensory processing, suggesting that feedforward information transfer in this frequency range is preserved.[33]

Importantly, as opposed to the effective connectivity approach based on perturbation of cortical networks through transcranial magnetic stimulation,[2,4,6] the information theoretic approach used in the current study reliably correlated with the behavioral quiescence during REM sleep, which is often associated with disconnected consciousness, i.e., dreams.[53,54] The consistent finding of disrupted frontal-parietal connectivity in the high gamma bandwidth across sleep and propofol/sevoflurane-induced unconsciousness provides further evidence that unconsciousness due to sleep and anesthesia might have shared cortical mechanisms.[55-57] Frontal-parietal high gamma connectivity consistently correlated with behavioral arousal and may therefore be involved in what has been referred to as “connected consciousness,” i.e., consciousness of environmental stimuli during wakefulness. Based on our past work relating network hub structure to directionality in brain and non-biological networks,[12] we propose that these changes in directed connectivity reflect shifts in network topology.

Relationship of cortical acetylcholine and corticocortical connectivity

Cholinergic neurons in the basal forebrain and laterodorsal/pedunculopontine tegmentum are part of the arousal-promoting circuitry.[35,58] Our data show a decrease in acetylcholine in PFC during propofol- and sevoflurane-induced unconsciousness, which recovered back to baseline levels during recovery from anesthesia. Similar findings have been reported by previous studies showing a decrease in acetylcholine across frontal cortex and in hippocampus during isoflurane, sevoflurane, and propofol anesthesia.[59-61] Cortical

acetylcholine levels are also known to be high during REM sleep, a state in which consciousness can occur in the absence of behavioral arousal.[35,40,53] As opposed to high gamma coherence and frontal-parietal connectivity, which correlated with the state of behavioral arousal, our data reveal that theta coherence and frontal-parietal connectivity in the theta bandwidth parallel levels of cortical acetylcholine. Therefore, cortical acetylcholine and theta connectivity correlate with an active cortex during wakefulness and REM sleep, rather than being associated with behavioral arousal. The dissociation between cortical acetylcholine and behavioral arousal is also supported by earlier reports that ablation of cholinergic neurons in basal forebrain either did not affect total wakefulness[62] or had a transient effect on wakefulness,[63] while systemic atropine produced a dissociated state with waking behavior in the presence of a slow wave electroencephalogram.[64] Conversely, cortical acetylcholine is increased after ketamine administration, despite the behavioral phenotype of general anesthesia.[29] Interestingly, the observed stepwise decrease in high gamma frontal-parietal directed connectivity across wakefulness, SWS, and REM sleep parallels progressive reduction in levels of cortical norepinephrine across sleep-wake cycle.[65] Furthermore, infusion of norepinephrine into basal forebrain under desflurane anesthesia in rats has been shown to produce microarousals along with increased cross-approximate entropy and decrease in frontal delta power,[66] while antagonism of norepinephrine in rat barrel cortex produced synaptic quiescence.[67] However, there has been no direct study of the role of cortical norepinephrine in frontal-parietal brain connectivity.

Limitations

A limitation of the current study is that we cannot draw causal conclusions regarding the relationships of cortical acetylcholine, behavioral arousal, and changes in electroencephalographic indices of connectivity. Furthermore, anesthetic induction and emergence are inherently unstable states and are particularly difficult to characterize in rodents, which makes it difficult to reliably quantify the neurochemical and neurophysiological changes during state transitions. Therefore, in order to identify correlates of clearly-defined states of consciousness, we focused on the most stable and representative epochs for anesthetic-induced unconsciousness. We acknowledge that the epochs of wakefulness we evaluated were states of complete wakefulness and thus the neural correlates identified might relate to cognition rather than consciousness, *per se*. As such, this investigation does not provide direct information regarding the transition points for states of wakefulness. However, unlike the many gradations along the continuum of sedation and general anesthesia that could have occurred between our data points, sleep and wakefulness are posited to discretely alternate or “flip-flop” across states.[68] Thus, the finding of impaired frontal-parietal connectivity during sleep states is supportive of observations during wakefulness and general anesthesia, despite the fact that transitions were not studied directly.

It is also important to note that, although our study assessed changes in corticocortical connectivity as correlates of wakefulness and anesthetic/sleep-induced unconsciousness, we cannot exclude important influences of the thalamus and/or basal forebrain through the ascending reticular activation system[21,55,58] on cortical activation and intra-cortical connectivity. Furthermore, in order to minimize the use of research animals and to avoid

redundancy, we relied on the previously published literature[35,40] and did not measure cortical acetylcholine during sleep-wake states.

Bioelectric potentials originating in muscle tissue are a known source of artifacts in scalp electroencephalographic data. In the current study, electroencephalogram was recorded using stainless steel electrodes directly implanted into the cranium. The electrodes were neither in physical contact with muscle tissues nor in close proximity (~3-4 mm away from nearest muscle tissue), and to our knowledge there is no preclinical rodent study showing interference from muscle tissues in the electroencephalographic data recorded using transcranial stainless steel electrodes. This issue was also addressed in a previous rat study (same electrodes, montage, and recording parameters) from our laboratory[28] and found no significant correlation of brain and muscle activity over a wide frequency range (0.1-250 Hz). However, a focused analysis to exclude completely the possibility of interference from muscle tissues in electroencephalographic data was not conducted in this study.

Conclusion

This is the first study to report suppression of electroencephalographic coherence and frontal-parietal directed connectivity in high gamma bandwidth across multiple states of unconsciousness (propofol anesthesia, sevoflurane anesthesia, SWS, REM sleep) compared with spontaneously occurring wakefulness. These data suggest that coherence and frontal-parietal connectivity in high gamma range are neural correlates of wakefulness and that the fragmentation of these oscillations might contribute to loss of behavioral arousal.

Supplementary Material

Refer to Web version on PubMed Central for supplementary material.

Acknowledgements

The authors thank Ralph Lydic, Ph.D. (Robert H. Cole Professor of Neuroscience, Department of Anesthesiology, University of Tennessee, Knoxville) for training and assistance with acetylcholine quantification. The authors also thank Chris Andrews, Ph.D. (Statistical Consultant, Center for Statistical Consultation and Research, University of Michigan Ann Arbor, Michigan) for help with statistical analysis, and Stella Wisidagamage, M.S. (Laboratory Technician, Department of Anesthesiology, University of Michigan, Ann Arbor, Michigan) for help with data collection.

Funding: This work was supported by a grant from the National Institutes of Health (Bethesda, MD, USA) to G.A.M (NIH R01 GM098578) and funding from the Department of Anesthesiology, University of Michigan Medical School, Ann Arbor.

References

1. Boveroux P, Vanhaudenhuyse A, Bruno MA, Noirhomme Q, Lauwick S, Luxen A, Degueldre C, Plenevaux A, Schnakers C, Phillips C, Brichant JF, Bonhomme V, Maquet P, Greicius MD, Laureys S, Boly M. Breakdown of within- and between-network resting state functional magnetic resonance imaging connectivity during propofol-induced loss of consciousness. Anesthesiology. 2010; 113:1038–53. [PubMed: 20885292]
2. Ferrarelli F, Massimini M, Sarasso S, Casali A, Riedner BA, Angelini G, Tononi G, Pearce RA. Breakdown in cortical effective connectivity during midazolam-induced loss of consciousness. Proc Natl Acad Sci U S A. 2010; 107:2681–86. [PubMed: 20133802]

3. Lewis LD, Weiner VS, Mukamel EA, Donoghue JA, Eskandar EN, Madsen JR, Anderson WS, Hochberg LR, Cash SS, Brown EN, Purdon PL. Rapid fragmentation of neuronal networks at the onset of propofol-induced unconsciousness. Proc Natl Acad Sci U S A. 2012; 109:E3377–86. [PubMed: 23129622]

4. Casali AG, Gosseries O, Rosanova M, Boly M, Sarasso S, Casali KR, Casarotto S, Bruno MA, Laureys S, Tononi G, Massimini M. A theoretically based index of consciousness independent of sensory processing and behavior. Sci Transl Med. 2013; 5:198ra05.

5. Schroeder KE, Irwin ZT, Gaidica M, Bentley JN, Patil PG, Mashour GA, Chestek CA. Disruption of corticocortical information transfer during ketamine anesthesia in the primate brain. Neuroimage. 2016; 134:459–65. [PubMed: 27095309]

6. Massimini M, Ferrarelli F, Huber R, Esser SK, Singh H, Tononi G. Breakdown of cortical effective connectivity during sleep. Science. 2005; 309:2228–32. [PubMed: 16195466]

7. Lee U, Kim S, Noh GJ, Choi BM, Hwang E, Mashour GA. The directionality and functional organization of frontoparietal connectivity during consciousness and anesthesia in humans. Conscious Cogn. 2009; 18:1069–78. [PubMed: 19443244]

8. Ku SW, Lee U, Noh GJ, Jun IG, Mashour GA. Preferential inhibition of frontal-to-parietal feedback connectivity is a neurophysiologic correlate of general anesthesia in surgical patients. PLoS ONE. 2011; 6:e25155. [PubMed: 21998638]

9. Jordan D, Ilg R, Riedl V, Schorer A, Grimberg S, Neufang S, Omerovic A, Berger S, Untergehrer G, Preibisch C, Schulz E, Schuster T, Schroter M, Spoormaker V, Zimmer C, Hemmer B, Wohlschlager A, Kochs EF, Schneider G. Simultaneous electroencephalographic and functional magnetic resonance imaging indicate impaired cortical top-down processing in association with anesthetic-induced unconsciousness. Anesthesiology. 2013; 119:1031–42. [PubMed: 23969561]

10. Lee H, Mashour GA, Noh GJ, Kim S, Lee U. Reconfiguration of network hub structure after propofol-induced unconsciousness. Anesthesiology. 2013; 119:1347–59. [PubMed: 24013572]

11. Lee U, Ku S, Noh G, Baek S, Choi B, Mashour GA. Disruption of frontal-parietal communication by ketamine, propofol, and sevoflurane. Anesthesiology. 2013; 118:1264–75. [PubMed: 23695090]

12. Moon JY, Lee U, Blain-Moraes S, Mashour GA. General relationship of global topology, local dynamics, and directionality in large-scale brain networks. PLoS Comput Biol. 2015; 11:e1004225. [PubMed: 25874700]

13. Raz A, Grady SM, Krause BM, Uhlrich DJ, Manning KA, Banks MI. Preferential effect of isoflurane on top-down vs. bottom-up pathways in sensory cortex. Front Syst Neurosci. 2014; 8:191. [PubMed: 25339873]

14. Boly M, Moran R, Murphy M, Boveroux P, Bruno MA, Noirhomme Q, Ledoux D, Bonhomme V, Brichant JF, Tononi G, Laureys S, Friston K. Connectivity changes underlying spectral EEG changes during propofol-induced loss of consciousness. J Neurosci. 2012; 32:7082–90. [PubMed: 22593076]

15. Monti MM, Lutkenhoff ES, Rubinov M, Boveroux P, Vanhaudenhuyse A, Gosseries O, Bruno MA, Noirhomme Q, Boly M, Laureys S. Dynamic change of global and local information processing in propofol-induced loss and recovery of consciousness. PLoS Comput Biol. 2013; 9:e1003271. [PubMed: 24146606]

16. Oizumi M, Albantakis L, Tononi G. From the phenomenology to the mechanisms of consciousness: Integrated Information Theory 3.0. PLoS Comput Biol. 2014; 10:e1003588. [PubMed: 24811198]

17. Godwin D, Barry RL, Marois R. Breakdown of the brain's functional network modularity with awareness. Proc Natl Acad Sci U S A. 2015; 112:3799–804. [PubMed: 25759440]

18. Murphy M, Bruno MA, Riedner BA, Boveroux P, Noirhomme Q, Landsness EC, Brichant JF, Phillips C, Massimini M, Laureys S, Tononi G, Boly M. Propofol anesthesia and sleep: a high-density EEG study. Sleep. 2011; 34:283–91A. [PubMed: 21358845]

19. Moore JT, Chen J, Han B, Meng QC, Veasey SC, Beck SG, Kelz MB. Direct activation of sleep-promoting VLPO neurons by volatile anesthetics contributes to anesthetic hypnosis. Curr Biol. 2012; 22:2008–16. [PubMed: 23103189]

20. Kottler B, Bao H, Zalucki O, Imlach W, Troup M, van Alphen B, Paulk A, Zhang B, van Swinderen B. A sleep/wake circuit controls isoflurane sensitivity in Drosophila. Curr Biol. 2013; 23:594–98. [PubMed: 23499534]
21. Baker R, Gent TC, Yang Q, Parker S, Vyssotski AL, Wisden W, Brickley SG, Franks NP. Altered activity in the central medial thalamus precedes changes in the neocortex during transitions into both sleep and propofol anesthesia. J Neurosci. 2014; 34:13326–35. [PubMed: 25274812]
22. Han B, McCarren HS, O'Neill D, Kelz MB. Distinctive recruitment of endogenous sleep-promoting neurons by volatile anesthetics and a nonimmobilizer. Anesthesiology. 2014; 121:999–1009. [PubMed: 25057841]
23. Liu X, Yanagawa T, Leopold DA, Chang C, Ishida H, Fujii N, Duyn JH. Arousal transitions in sleep, wakefulness, and anesthesia are characterized by an orderly sequence of cortical events. Neuroimage. 2015; 116:222–31. [PubMed: 25865143]
24. Zalucki O, Day R, Kottler B, Karunanithi S, van Swinderen B. Behavioral and electrophysiological analysis of general anesthesia in 3 background strains of Drosophila melanogaster. Fly. 2015; 9:7–15. [PubMed: 26267354]
25. Zhang Z, Ferretti V, Guntan I, Moro A, Steinberg EA, Ye Z, Zecharia AY, Yu X, Vyssotski AL, Brickley SG, Yustos R, Pillidge ZE, Harding EC, Wisden W, Franks NP. Neuronal ensembles sufficient for recovery sleep and the sedative actions of alpha2 adrenergic agonists. Nat Neurosci. 2015; 18:553–61. [PubMed: 25706476]
26. Hudetz AG. General anesthesia and human brain connectivity. Brain Connect. 2012; 2:291–302. [PubMed: 23153273]
27. Paxinos, G.; Watson, C. The Rat Brain in Sterotaxic Coordinates. 6th edition. Academic Press; London: 2007.
28. Borjigin J, Lee U, Liu T, Pal D, Huff S, Klarr D, Sloboda J, Hernandez J, Wang MM, Mashour GA. Surge of neurophysiological coherence and connectivity in the dying brain. Proc Natl Acad Sci U S A. 2013; 110:14432–37. [PubMed: 23940340]
29. Pal D, Hambrecht-Wiedbusch VS, Silverstein B, Mashour GA. Electroencephalographic cohearence and cortical acetylcholine during ketamine-induced unconsciousness. Br J Anaesth. 2015; 114:979–89. [PubMed: 25951831]
30. Nicolaou N, Georgiou J. Global field synchrony during general anaesthesia. Br J Anaesth. 2014; 112:529–39. [PubMed: 24169819]
31. Cavinato M, Genna C, Manganotti P, Formaggio E, Storti SF, Campostrini S, Arcaro C, Casanova E, Petrone V, Piperno R, Piccione F. Coherence and consciousness: study of fronto-parietal gamma synchrony in patients with disorders of consciousness. Brain Topogr. 2015; 28:570–79. [PubMed: 25070585]
32. Schreiber T, Schmitz A. Surrogate time series. Physica D Nonlinear Phenomena. 2000; 142:346–82.
33. Imas OA, Ropella KM, Ward BD, Wood JD, Hudetz AG. Volatile anesthetics disrupt frontal-posterior recurrent information transfer at gamma frequencies in rat. Neurosci Lett. 2005; 387:145–50. [PubMed: 16019145]
34. Wollstadt P, Sellers KK, Hutt A, Frohlich F, Wibral M. Anesthesia-related changes in information transfer may be caused by reduction in local information generation. Conf Proc IEEE Eng Med Biol Soc. 2015; 2015:4045–48. [PubMed: 26737182]
35. Lydic R, Baghdoyan HA. Sleep, anesthesiology, and the neurobiology of arousal state control. Anesthesiology. 2005; 103:1268–95. [PubMed: 16306742]
36. Naghavi HR, Nyberg L. Common fronto-parietal activity in attention, memory, and consciousness: shared demands on integration? Conscious Cogn. 2005; 14:390–425. [PubMed: 15950889]
37. Osman NI, Baghdoyan HA, Lydic R. Morphine inhibits acetylcholine release in rat prefrontal cortex when delivered systemically or by microdialysis to basal forebrain. Anesthesiology. 2005; 103:779–87. [PubMed: 16192770]
38. Brown EN, Lydic R, Schiff ND. General anesthesia, sleep, and coma. N Engl J Med. 2010; 363:2638–50. [PubMed: 21190458]

39. Vanini G, Nemanis K, Baghdoyan HA, Lydic R. GABAergic transmission in rat pontine reticular formation regulates the induction phase of anesthesia and modulates hyperalgesia caused by sleep deprivation. Eur J Neurosci. 2014; 40:2264–73. [PubMed: 24674578]
40. Marrosu F, Portas C, Mascia MS, Casu MA, Fa M, Giagheddu M, Imperato A, Gessa GL. Microdialysis measurement of cortical and hippocampal acetylcholine release during sleep-wake cycle in freely moving cats. Brain Res. 1995; 671:329–32. [PubMed: 7743225]
41. Buzsaki G, Wang XJ. Mechanisms of gamma oscillations. Annu Rev Neurosci. 2012; 35:203–25. [PubMed: 22443509]
42. Sohal VS. Insights into cortical oscillations arising from optogenetic studies. Biol Psychiatry. 2012; 71:1039–45. [PubMed: 22381731]
43. Bosman CA, Lansink CS, Pennartz CM. Functions of gamma-band synchronization in cognition: from single circuits to functional diversity across cortical and subcortical systems. Eur J Neurosci. 2014; 39:1982–99. [PubMed: 24809619]
44. Desmedt JE, Tomberg C. Transient phase-locking of 40 Hz electrical oscillations in prefrontal and parietal human cortex reflects the process of conscious somatic perception. Neurosci Lett. 1994; 168:126–29. [PubMed: 8028764]
45. Rodriguez E, George N, Lachaux JP, Martinerie J, Renault B, Varela FJ. Perception's shadow: long-distance synchronization of human brain activity. Nature. 1999; 397:430–33. [PubMed: 9989408]
46. Melloni L, Molina C, Pena M, Torres D, Singer W, Rodriguez E. Synchronization of neural activity across cortical areas correlates with conscious perception. J Neurosci. 2007; 27:2858–65. [PubMed: 17360907]
47. Uhlhaas PJ, Pipa G, Neuenschwander S, Wibral M, Singer W. A new look at gamma? High- (>60 Hz) gamma-band activity in cortical networks: function, mechanisms and impairment. Prog Biophys Mol Biol. 2011; 105:14–28. [PubMed: 21034768]
48. Imas OA, Ropella KM, Wood JD, Hudetz AG. Isoflurane disrupts anterio-posterior phase synchronization of flash-induced field potentials in the rat. Neurosci Lett. 2006; 402:216–21. [PubMed: 16678343]
49. John ER, Prichep LS, Kox W, Valdes-Sosa P, Bosch-Bayard J, Aubert E, Tom M, di Michele F, Gugino LD. Invariant reversible QEEG effects of anesthetics. Conscious Cogn. 2001; 10:165–83. [PubMed: 11414713]
50. Castro S, Falconi A, Chase MH, Torterolo P. Coherent neocortical 40-Hz oscillations are not present during REM sleep. Eur J Neurosci. 2013; 37:1330–39. [PubMed: 23406153]
51. Castro S, Cavelli M, Vollono P, Chase MH, Falconi A, Torterolo P. Inter-hemispheric coherence of neocortical gamma oscillations during sleep and wakefulness. Neurosci Lett. 2014; 578:197–202. [PubMed: 24993304]
52. Cavelli M, Castro S, Schwarzkopf N, Chase MH, Falconi A, Torterolo P. Coherent neocortical gamma oscillations decrease during REM sleep in the rat. Behav Brain Res. 2015; 281:318–25. [PubMed: 25557796]
53. Hobson JA. REM sleep and dreaming: towards a theory of protoconsciousness. Nat Rev Neurosci. 2009; 10:803–13. [PubMed: 19794431]
54. Voss U, Holzmann R, Tuin I, Hobson JA. Lucid dreaming: a state of consciousness with features of both waking and non-lucid dreaming. Sleep. 2009; 32:1191–200. [PubMed: 19750924]
55. Franks NP. General anaesthesia: from molecular targets to neuronal pathways of sleep and arousal. Nat Rev Neurosci. 2008; 9:370–86. [PubMed: 18425091]
56. Pal D, Lipinski WJ, Walker AJ, Turner AM, Mashour GA. State-specific effects of sevoflurane anesthesia on sleep homeostasis: selective recovery of slow wave but not rapid eye movement sleep. Anesthesiology. 2011; 114:302–10. [PubMed: 21239972]
57. Tung A, Bergmann BM, Herrera S, Cao D, Mendelson WB. Recovery from sleep deprivation occurs during propofol anesthesia. Anesthesiology. 2004; 100:1419–26. [PubMed: 15166561]
58. Jones BE. From waking to sleeping: neuronal and chemical substrates. Trends Pharmacol Sci. 2005; 26:578–86. [PubMed: 16183137]

59. Shichino T, Murakawa M, Adachi T, Arai T, Miyazaki Y, Mori K. Effects of inhalation anaesthetics on the release of acetylcholine in the rat cerebral cortex in vivo. Br J Anaesth. 1998; 80:365–70. [PubMed: 9623440]

60. Kikuchi T, Wang Y, Sato K, Okumura F. In vivo effects of propofol on acetylcholine release from the frontal cortex, hippocampus and striatum studied by intracerebral microdialysis in freely moving rats. Br J Anaesth. 1998; 80:644–48. [PubMed: 9691870]

61. Nemoto C, Murakawa M, Hakozaki T, Imaizumi T, Isosu T, Obara S. Effects of dexmedetomidine, midazolam, and propofol on acetylcholine release in the rat cerebral cortex in vivo. J Anesth. 2013; 27:771–74. [PubMed: 23483299]

62. Blanco-Centurion C, Gerashchenko D, Shiromani PJ. Effects of saporin-induced lesions of three arousal populations on daily levels of sleep and wake. J Neurosci. 2007; 27:14041–48. [PubMed: 18094243]

63. Kaur S, Junek A, Black MA, Semba K. Effects of ibotenate and 192IgG-saporin lesions of the nucleus basalis magnocellularis/substantia innominata on spontaneous sleep and wake states and on recovery sleep after sleep deprivation in rats. J Neurosci. 2008; 28:491–504. [PubMed: 18184792]

64. Qiu MH, Chen MC, Lu J. Cortical neuronal activity does not regulate sleep homeostasis. Neuroscience. 2015; 297:211–18. [PubMed: 25864961]

65. Aston-Jones G, Bloom FE. Activity of norepinephrine-containing locus coeruleus neurons in behaving rats anticipates fluctuations in the sleep-waking cycle. J Neurosci. 1981; 1:876–86. [PubMed: 7346592]

66. Pillay S, Vizuete JA, McCallum JB, Hudetz AG. Norepinephrine infusion into nucleus basalis elicits microarousal in desflurane-anesthetized rats. Anesthesiology. 2011; 115:733–42. [PubMed: 21804378]

67. Constantinople CM, Bruno RM. Effects and mechanisms of wakefulness on local cortical networks. Neuron. 2011; 69:1061–68. [PubMed: 21435553]

68. Lu J, Sherman D, Devor M, Saper CB. A putative flip-flop switch for control of REM sleep. Nature. 2006; 441:589–94. [PubMed: 16688184]

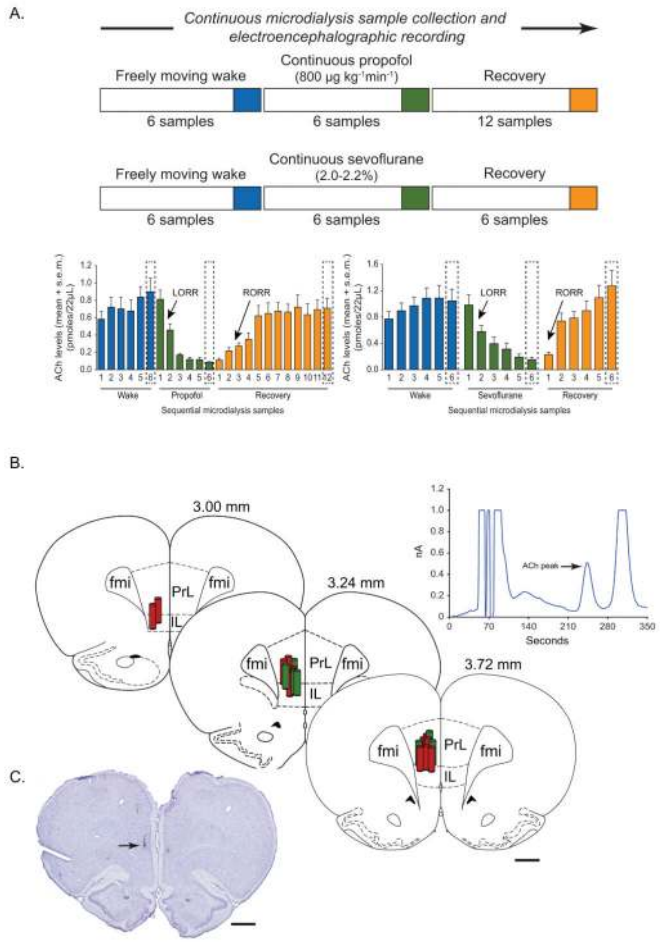

Figure 1.

A) Schematic illustrating the design for microdialysis experiments and temporal course of electroencephalogram and acetylcholine (ACh) data collection. Each ACh sample epoch represents microdialysate collected over a period of 12.5 min. The electroencephalographic data were analyzed in the corresponding 12.5 min epochs. Blue, green and orange bars represent wake, anesthetic-induced unconsciousness (propofol/sevoflurane), and post-anesthetic recovery wake epochs, respectively. The epochs highlighted with broken lines were selected for statistical comparisons. Arrows indicate the approximate time points at which rats showed loss of righting reflex (LORR) and recovery of righting reflex (RORR). B) Reconstruction diagram shows a cascade of coronal brain section drawings from the rat brain atlas[27] to illustrate the location (vertical cylinders) of microdialysis probes (1 mm) within the prefrontal cortex. Green cylinders represent the microdialysis probes from the propofol experiments while the red cylinders represent those from the sevoflurane experiments. Numbers above the coronal brain section drawings are the anterior-posterior stereotaxic coordinates relative to Bregma. The chromatogram above the reconstruction diagram shows signal to noise ratio and the retention time for ACh. C) Cresyl violet stained representative coronal brain section through prefrontal cortex shows the dialysis probe track and the site of microdialysis. Arrow indicates the location of ventral tip of the microdialysis

membrane. fmi - forceps minor corpus callosum, IL - infralimbic area, PrL - prelimbic area. Scale bar - 1 mm.

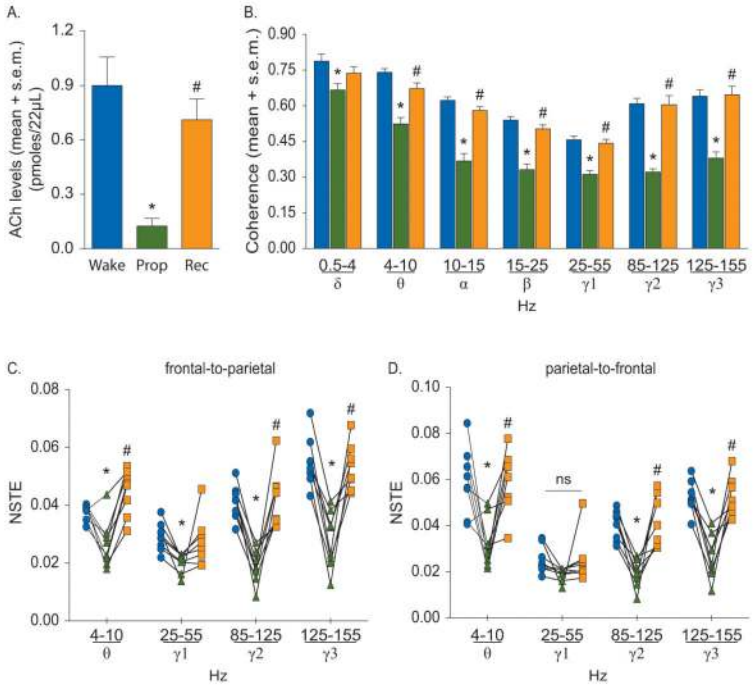

Figure 2.

Effect of propofol on cortical acetylcholine (ACh) (A), corticocortical coherence (B), and frontal-parietal directed connectivity (C-D). The symbol-line plots (C-D) show the individual rat data while the significance symbols represent the outcome of group level statistical testing using repeated measures analysis of variance with Tukey's multiple comparisons test. Significance symbols denote a statistical difference at an alpha of $p<0.05$. The actual p values are reported in the text in the results section. *significant as compared to wake, #significant as compared to propofol-induced unconsciousness, blue bars/circles: wake, green bars/triangles: propofol-induced unconsciousness, orange bars/squares: post-propofol recovery wake. ns: not significant, NSTE: normalized symbolic transfer entropy, Prop: propofol, Rec: recovery wake, s.e.m.: standard error of the mean.

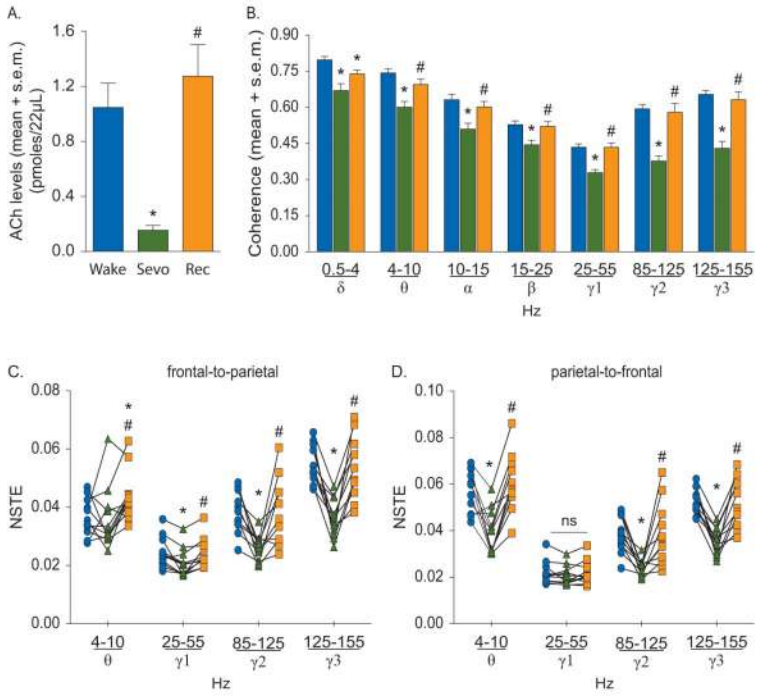

Figure 3.

Effect of sevoflurane on cortical acetylcholine (ACh) (A), corticocortical coherence (B), and frontal-parietal directed connectivity (C-D). The symbol-line plots (C-D) show the individual rat data while the significance symbols represent the outcome of group level statistical testing using repeated measures analysis of variance with Tukey's multiple comparisons test. Significance symbols denote a statistical difference at an alpha of $p<0.05$. The actual p values are reported in the text in the results section. *significant as compared to wake, #significant as compared to sevoflurane-induced unconsciousness, blue bars/circles: wake, green bars/triangles: sevoflurane-induced unconsciousness, orange bars/squares: post-sevoflurane recovery wake. ns: not significant, NSTE: normalized symbolic transfer entropy, Rec: recovery wake, s.e.m.: standard error of the mean, Sevo: sevoflurane.

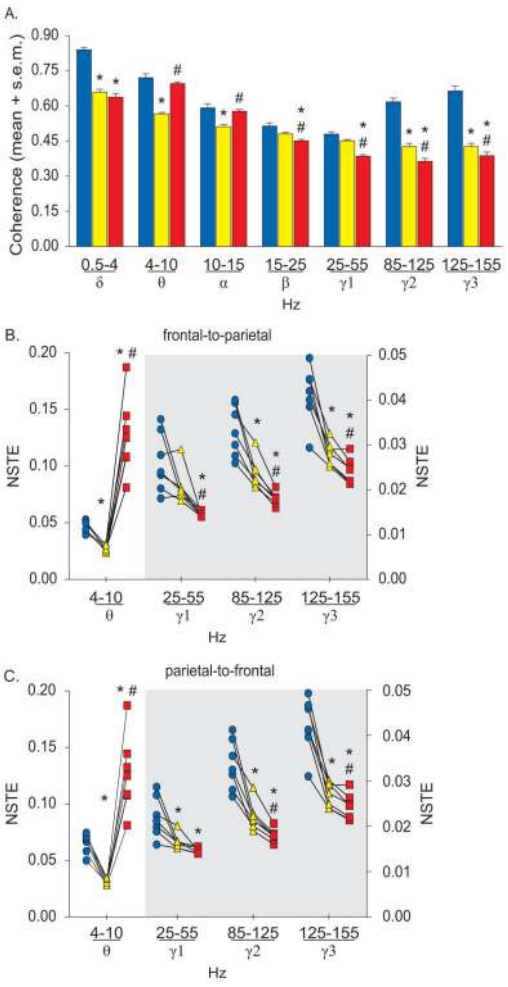

Figure 4.

Corticocortical coherence (A) and frontal-parietal directed connectivity (B-C) during wakefulness, slow wave sleep, and rapid eye movement sleep. The symbol-line plots (B-C) show the individual rat data while the significance symbols represent the outcome of group level statistical testing using repeated measures analysis of variance with Tukey's multiple comparisons test. The right axis in (B) and (C) applies only to the grey shaded area. Significance symbols denote a statistical difference at an alpha of $p<0.05$. The actual p values are reported in the text in the results section. *significant as compared to wake, #significant as compared to slow wave sleep, blue bars/circles: wake, yellow bars/ triangles: slow wave sleep, red bars/squares: rapid eye movement sleep. NSTE: normalized symbolic transfer entropy, s.e.m.: standard error of the mean.

Table 1

Relationship between electroencephalogram (EEG), cortical acetylcholine (ACh), states of arousal, and frontal-parietal directed connectivity in theta (θ) and high gamma (γ: 85-155 Hz) bandwidth. Coherence and frontal-parietal high gamma connectivity were disrupted during all states of behavioral unconsciousness, i.e., propofol/sevoflurane-induced unconsciousness, slow wave sleep, and rapid eye movement sleep. Slow EEG indicates high-amplitude/slow-wave EEG, Activated/fast EEG indicates low-amplitude/fast-wave EEG.

	Unconscious states				Wakefulness		
	Propofol	**Sevoflurane**	**Slow wave sleep**	**Rapid eye movement sleep**	**Spontaneous wakefulness**	**Post-Propofol recovery wake**	**Post-Sevoflurane recovery wake**
EEG	Slow	Slow	Slow	Activated/fast	Activated/fast	Activated/fast	Activated/fast
Cortical ACh	Low	Low	Low	High	High	High	High
θ Coherence	Low	Low	Low	High	High	High	High
θ Frontal-to-parietal connectivity	Low	Not Affected	Low	High	High	High	High
θ Parietal-to-frontal connectivity	Low	Low	Low	High	High	High	High
γ Coherence	Low	Low	Low	**Low**	High	High	High
γ Frontal-to-parietal connectivity	Low	Low	Low	**Low**	High	High	High
γ Parietal-to-frontal connectivity	Low	Low	Low	**Low**	High	High	High

Anesthesiology. Author manuscript; available in PMC 2017 November 01.